Determination of spectral linewidths by Voigt profiles in Yb^{3+}-doped fluorozirconate glasses

G. Lei, J. E. Anderson, M. I. Buchwald, B. C. Edwards, and R. I. Epstein
Los Alamos National Laboratory, Los Alamos, New Mexico 87545
(Received 12 August 1997; revised manuscript received 20 November 1997)

Homogeneous and inhomogeneous spectral linewidths of the $(^2F_{5/2})_1-(^2F_{7/2})_1$ transition in Yb^{3+}-doped fluorozirconate glasses are determined by fitting Voigt profiles to the inhomogeneously broadened emission and absorption spectra between 10 and 300 K. The homogeneous linewidth varied as $(12\pm2)\times T^{(1.9\pm0.1)}$ MHz for emission and $(10\pm1)\times T^{1.9\pm0.1}$ for absorption over the entire temperature range, similar to that of other rare-earth-doped systems previously studied by fluorescence line narrowing and photon echoes. The inhomogeneous linewidths were nearly independent of temperature, but different by ~30% between emission and absorption. The structural and dynamic properties in this disordered system are discussed. [S0163-1829(98)00614-6]

I. INTRODUCTION

The optical linewidths of ions in glasses are of considerable interest as a probe of the structural and dynamic properties of the amorphous state. The interest has been spurred by the observation of homogeneous linewidths that have an anomalously large magnitude and that exhibit an unusual temperature dependence, as compared with that of their crystalline counterparts. The data at low temperature ($T<10$ K) show linear and $T^{1.3}$ dependencies.[1] This behavior has been ascribed to the two-level systems (TLS) (Ref. 2) invoked to account phenomenologically for the anomalous heat capacity and thermal conductivity of amorphous systems.[3,4] A T^2 dependence at high temperature is attributed to two-phonon processes, as in crystalline hosts, to which all thermally accessible phonons contribute when $T>0.5T_D$, where T_D is the Debye temperature.[5,6] The intermediate temperature regime remains elusive both theoretically and experimentally.

In this intermediate temperature region, a nearly T^2 dependence of homogeneous linewidth is commonly measured for various combinations of ions and glassy hosts,[1] including trivalent europium[7] and curium[8] ions in fluorozirconate glasses. Exceptions are trivalent ytterbium ions in phosphate glass[9] and a recent study on trivalent europium ions in fluorophosphate glass.[10] One would expect a crossover between the mechanism that dominates at high temperature (i.e., two-phonon processes) to that active at low temperature (e.g., TLS's). That is, there should be a crossover between the T^2 behavior at high temperature and a linear or $T^{1.3}$ behavior at low temperature.

Optical transitions of ions in glasses are inhomogeneously broadened due to site-to-site variations of the local crystal fields. For a given transition the homogeneous Lorentzian line shapes are convoluted with an inhomogeneous Gaussian distribution in energy eigenvalues. The homogeneous linewidths have been measured by experimental techniques that eliminate the effects of the inhomogeneous broadening to determine the homogeneous widths; these include fluorescence line narrowing (FLN) (Ref. 11) and spectral hole burning[12] in the frequency domain, and photon echoes[13] in the time domain. In the fluorescence line narrowing measurements, for example, a narrow band laser, whose width is small compared to the homogeneous width, is employed to excite a small subset of ions within the inhomogeneous profile, and the observation is made rapidly, before energy transfer and the resultant spectral diffusion occur. In general these techniques may feature different time scales and measure different physical quantities, which lead to different temperature limitations. The fluorescence line narrowing technique, for example, runs into difficulty at low-temperature when the measured linewidth is smaller than the laser bandwidth. Spectral hole burning and photon echoes have problems at high temperature where holes are not burned efficiently and the dephasing time becomes comparable with the laser pulse width. There is a need for a technique capable of spanning a wide temperature range so that more extensive studies on a system can be made by the single technique.

We present here a study of spectral linewidth in a glass by fitting the inhomogeneously broadened equilibrium emission and white-light absorption spectra to Voigt profiles to extract the homogeneous and inhomogeneous components. This deconvolution technique can span a large range of temperature and measures both homogeneous and inhomogeneous widths at the same time. It works well as long as the transition peak being studied is well resolved. We discuss the linewidths and their temperature dependence that provide important information on structure and dynamics of the disordered system.

II. EXPERIMENTAL RESULTS AND ANALYSIS

Heavy-metal fluoride glasses have been widely investigated for the purpose of developing laser hosts, optical fibers, and new optical devices such as optical refrigerators.[14] The interest has been stimulated by their low intrinsic losses, e.g., low nonradiative relaxation rates,[15] and a wide range of transparency ($0.2-7\ \mu$m), which is a consequence of the low phonon energies ($\sim500\ \text{cm}^{-1}$) in these materials. The glass sample we investigated was a Yb^{3+}-doped fluorozirconate glass ZBLANP, with the composition of 51.8% ZrF_4, 19.5% BaF_2, 4.7% LaF_3, 3.2% AlF_3, 18.3% NaF, 2.5% PbF_2, and 1% YbF_3. The fluorozirconate glasses have an uncommon structure, based on the network former ZrF_4, described by a three-dimensional random network of polyhedra with a high degree of coordination. The Yb^{3+} ion has a

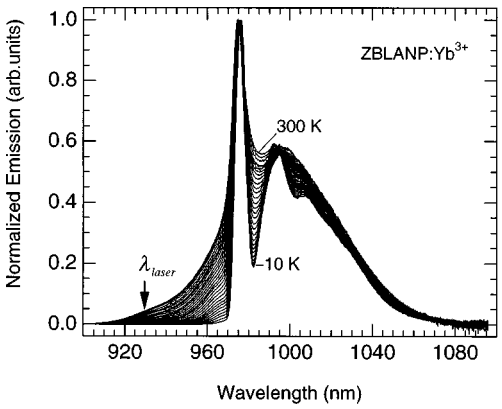

FIG. 1. The emission spectra from 10 to 300 K, the temperature intervals between the curves shown are about ~12 K for $10<T<100$ K, and ~10 K for $100<T<300$ K. The curves were normalized at the peak $(^2F_{5/2})_1 \rightarrow (^2F_{7/2})_1$ near ~975 nm.

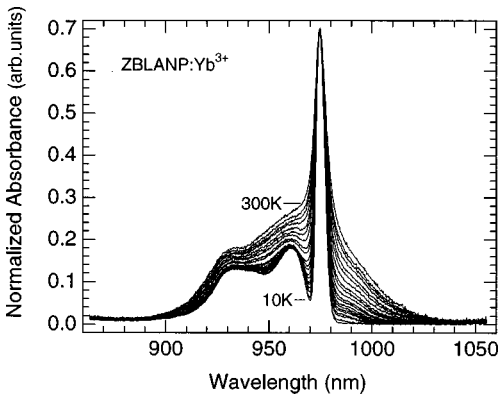

FIG. 2. The absorption spectra from 10 to 300 K, the temperature intervals between the curves are similar to Fig. 1. The curves were normalized at the peak.

simple $4f^{13}$ electronic structure consisting of a ground state $^2F_{7/2}$ and an excited state $^2F_{5/2}$, separated by ~10 000 cm^{-1}, with moderately strong electric-dipole transitions. In ZBLANP glasses, the Yb^{3+} ions occupy sites of low enough symmetry to completely lift the Stark degeneracy except for the Kramers degeneracy.[16] The upper manifold splits to three levels and the lower to four.

The emission measurements were made using a tunable cw Ti:Sapphire laser (Spectra-Physics Model 3900 S) pumped with an Ar^+ laser (Coherent INNOVA 20). The output power was ~50 mW with a spectral bandwidth ≤30 GHz. A sample was placed in a cryostat (Infrared Lab. HDL-8) and the temperature was measured with a calibrated silicon diode. A fused silica optic fiber bundle directs the fluorescence to the entrance slit of the monochromator, a Digikröm 240 (CVI Laser Co.) equipped with a charge-coupled device (CCD) array detector (Santa Barbara ST-6). The emission spectra were corrected for the CCD response and the attenuation of the fused silica fiber. Because of the strong absorption from the ground state of the $^2F_{7/2}$ manifold, the emission is subject to radiation trapping in the sample that distorts the fluorescence spectrum. This was reduced by using a small sample and pumping near the surface that is observed. The fluorescence spectra of the $^2F_{5/2} \rightarrow {}^2F_{7/2}$ transitions of Yb^{3+} as a function of temperature are shown in Fig. 1. The curves were normalized at the peak $(^2F_{5/2})_1 \rightarrow (^2F_{7/2})_1$ near ~975 nm, which narrows with decreasing temperature. The laser spike at 930 nm has been removed from the spectra. The inhomogeneous broadening of the intraconfigurational transitions is comparable to the Stark splitting, and masks much of the structure even at low temperature. Only the zero-line $(^2F_{5/2})_1 \rightarrow (^2F_{7/2})_1$, the transition between the lowest Stark-levels of the $^2F_{7/2}$ and $^2F_{5/2}$ manifolds, is clearly resolved. The other three $(^2F_{5/2})_1 \rightarrow (^2F_{7/2})_{2,3,4}$ transitions are just barely resolvable even at low temperature, and merge into a featureless broad band as the temperature increases.

The absorption measurements were made with a similar setup, a calibrated white-light source replaced the laser. The sample was placed in the cryostat mounted on a micrometer stage. The transmission I_t and reference I_0 spectra were taken by moving the Dewar container slightly such that the white-light beam passes through the sample for transmission and past the sample for reference. This is to minimize any changes in window reflection losses. Figure 2 shows the temperature dependence of absorption spectra, where the absorbance is $\ln(I_0/I_t)$. The curves were normalized at the peak $(^2F_{7/2})_1 \rightarrow (^2F_{5/2})_1$ near ~975 nm.

The overall width of emission and absorption lines in glassy hosts is due to two effects, homogeneous and inhomogeneous broadening. Homogeneous broadening, from dynamic perturbations on energy levels and equally on all ions, leads to a Lorentzian line shape $g_L(\nu)$ of width $\Delta\nu_L$. Inhomogeneous broadening, due to site variation produced by a random distribution of local crystal fields, results in a Gaussian line shape $g_G(\nu)$ of width $\Delta\nu_G$. Since inhomogeneous broadening is not strongly correlated on different optical transitions,[17] the observed spectral line shapes may be described by the convolution of these two, i.e., a Voigt profile:[18,19]

$$g_V(\nu)=\int_{-\infty}^{+\infty} g_G(\nu')g_L(\nu-\nu')d\nu'=\frac{\sqrt{\ln 2/\pi}}{\Delta\nu_G}K(x,y), \tag{1}$$

where the Voigt function is

$$K(x,y)=\frac{y}{\pi}\int_{-\infty}^{+\infty}\frac{e^{-z^2}}{y^2+(x-z)^2}\,dz, \tag{2}$$

and $x=\sqrt{\ln 2}(\nu-\nu_0)/\Delta\nu_G$, $y=\sqrt{\ln 2}\Delta\nu_L/\Delta\nu_G$ are dimensionless variables and ν_0 is the line center frequency. The convolution integral is computed numerically, and the numerical fits to the data were carried out by a data analysis program (IGOR, Wavemetrics, Inc.). The algorithm used is patterned after Humlicek,[20] and discussed by Schreier.[19] Figure 3 shows four Voigt peaks fit to the emission spectra at 10 K. At this temperature, the levels $(^2F_{5/2})_{2,3}$ have very low populations and the emission is predominantly from the $(^2F_{5/2})_1 \rightarrow (^2F_{7/2})_{1,2,3,4}$ transitions. The baselines of the spectra were fit with cubic polynomials. The line shape of the $(^2F_{5/2})_1 \rightarrow (^2F_{7/2})_1$ transition is well resolved, and we were able to accurately deconvolute the homogeneous and inhomogeneous components of the line. Because the three $(^2F_{5/2})_1 \rightarrow (^2F_{7/2})_{2,3,4}$ transitions are so heavily overlapped, however, the deconvolution failed to give a definitive result

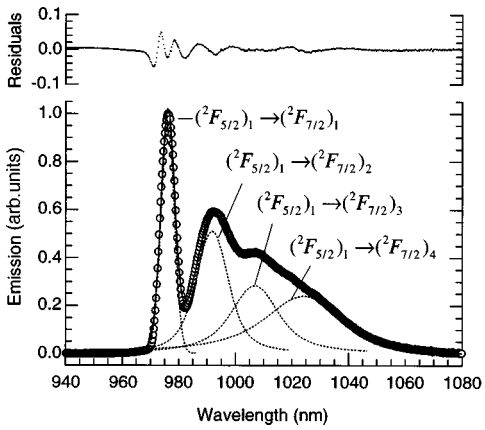

FIG. 3. Four Voigt profiles fit to the emission spectra of the $(^2F_{5/2})_1 \rightarrow (^2F_{7/2})_{1,2,3,4}$ transitions of Yb^{3+} at 10 K. The four dotted-line peaks correspond to the transitions of the lowest Stark level of the upper manifold to the four levels of the lower manifold.

for the homogeneous and inhomogeneous components of the individual peaks of this band; even at low temperature where the three transitions were just barely resolved, only the line center positions are significant. These line shapes could not be fit uniquely. The absorption spectra at 100 K shown in Fig. 4 were similarly fit. The $(^2F_{7/2})_1 \rightarrow (^2F_{5/2})_1$ transition is well resolved, and we reliably deconvolute the shape of this single peak. The $(^2F_{7/2})_1 \rightarrow (^2F_{5/2})_{2,3}$ transitions could not be fitted in a definitive way. Both homogeneous and inhomogeneous linewidths of the $(^2F_{5/2})_1 - (^2F_{7/2})_1$ emission and absorption lines are shown in Figs. 5 and 6. The homogeneous widths exhibit a simple power law dependence on temperature over the entire temperature range in both the emission and the absorption. The solid lines is the power law fit to the data, which give $\Delta\nu_L \sim (12\pm2)\times T^{(1.9\pm0.1)}$ (MHz) for the emission and $\Delta\nu_L \sim (10\pm1)\times T^{(1.9\pm0.1)}$ (MHz) for the absorption. The inhomogeneous widths are largely independent of temperature with a mean value of $\Delta\overline{\nu}_G \sim (990\pm40)$ (GHz) ($\sim 33.1\pm1.4\ \mathrm{cm}^{-1}$) for the emission, and $\Delta\overline{\nu}_G \sim (709\pm20)$ (GHz) ($\sim 23.6\pm0.6\ \mathrm{cm}^{-1}$) for the absorption. The results of the Voigt profile fits depend, to some extent, on the initial values chosen. This leads to an uncertainty in the homogeneous linewidths of $\leqslant 50\%$ for each observation. This uncertainty has been included in our parameter estimations.

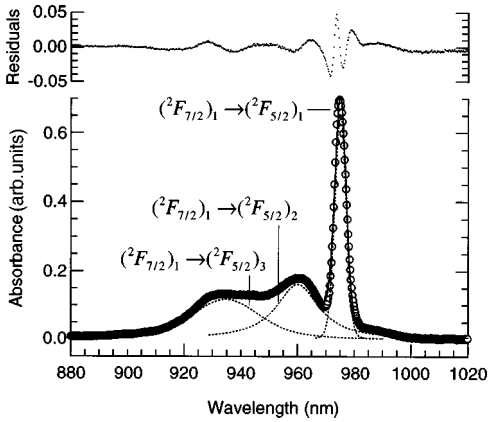

FIG. 4. Three Voigt profiles fit to the absorption spectra of the $(^2F_{7/2})_1 \rightarrow (^2F_{5/2})_{1,2,3}$ transitions in Yb^{3+} at 100 K. The three dotted-line peaks correspond to the transitions of the lowest Stark level of lower manifold to the three levels of upper manifold.

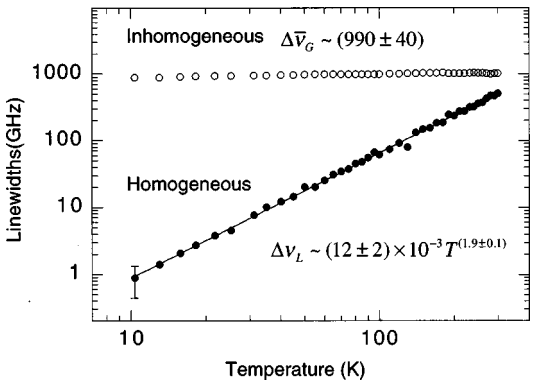

FIG. 5. Log-log plot of homogeneous and inhomogeneous widths of the $(^2F_{5/2})_1 \rightarrow (^2F_{7/2})_1$ transition in emission spectra as a function of temperature. The solid line is the quadratic fit to the data, and the error bar shows a representative fitting uncertainty in the homogeneous width.

III. DISCUSSION

A. Homogeneous linewidths

The homogeneous widths of $(12\pm2)\times T^{(1.9\pm0.1)}$ (MHz) in emission are close to that of $(10\pm1)\times T^{(1.9\pm0.1)}$ (MHz) in absorption, and both sets are similar to those of other rare-earth-doped systems studied by fluorescence line narrowing and photon echoes techniques. To compare with previous results, Table I lists some studies of homogeneous linewidths in rare earth-doped glass systems. The first two entries are the data presented here. The second group (rows 3–9) includes studies of nonfluoride glasses at temperature ranges overlapping with ours; both the magnitude and the temperature dependence of these homogeneous linewidths are similar to our results. Homogeneous linewidth data of trivalent ytterbium ion in fluorozirconate glasses are not available for a direct comparison. For the fluorozirconate glassy hosts, the third group (rows 10, 11), our results are somewhat smaller than $14.8\times T^{1.95}$ measured for trivalent curium in ZBLAN,[8] but about 10 times larger than $1.2\times T^2$ for trivalent europium

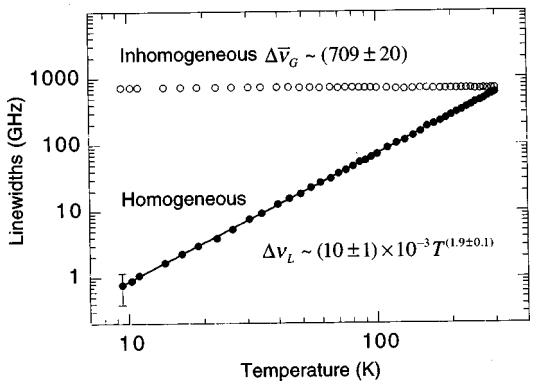

FIG. 6. Log-log plot of homogeneous and inhomogeneous widths of the $(^2F_{7/2})_1 \rightarrow (^2F_{5/2})_1$ transition in absorption spectra as a function of temperature. The solid line is the quadratic fit to the data, and the error bar shows a representative fitting uncertainty in the homogeneous width.

TABLE I. Homogeneous linewidths of selected trivalent lanthanide and actinide-doped inorganic glasses.

Row	Host glasses	Ions	Transitions	Linewidths (MHz)	Temp. range (K)	Techniques[a]	Ref.
1	ZBLANP	Yb^{3+}	$(^2F_{5/2})_1 \rightarrow (^2F_{7/2})_1$	$12\times T^{1.9\pm0.1}$	10∼300	Equilibrium fluorescence	This work
2	ZBLANP	Yb^{3+}	$(^2F_{7/2})_1 \rightarrow (^2F_{5/2})_1$	$10\times T^{1.9\pm0.1}$	10∼300	White-light absorption	This work
3	GeO_2	Pr^{3+}	$^3P_0 \rightarrow (^3H_4)_1$	$15.2\times T^{1.9\pm0.2}$	8∼300	FLN	5
4	Li-Silicate	Eu^{3+}	$^5D_0 \rightarrow {}^7F_0$	$4.8\times T^2$	10∼300	FLN	27
5	Na-Silicate	Eu^{3+}	$^5D_0 \rightarrow {}^7F_0$	$3.4\times T^2$	10∼300	FLN	27
6	K-Germanate	Eu^{3+}	$^5D_0 \rightarrow {}^7F_0$	$3.4\times T^2$	10∼300	FLN	27
7	Silicate	Eu^{3+}	$^5D_0 \rightarrow {}^7F_0$	$13\times T^{1.8\pm0.2}$	8∼90	FLN	11
8	Phosphate	Nd^{3+}	$^4I_{9/2} \rightarrow {}^7F_{3/2}$	$29.2\times T^{1.9}$	80∼210	FLN	6
9	Silicate	Nd^{3+}	$^4I_{9/2} \rightarrow {}^7F_{3/2}$	$3\times T^{2.2}$	10∼100	PE	13
10	ZBLA	Eu^{3+}	$^5D_0 \rightarrow {}^7F_0$	$1.2\times T^2$	10∼160	FLN	7
11	ZBLAN	Cm^{3+}	$^6D_{7/2} \rightarrow {}^8S_{7/2}$	$14.8\times T^{1.95}$	15∼100	FLN	8
12	Phosphate	Yb^{3+}	$(^2F_{5/2})_1 \rightarrow (^2F_{7/2})_1$	$15\times T^{1.3}$	6.5∼40	FLN	9
13	Phosphate	Yb^{3+}	$(^2F_{5/2})_1 \rightarrow (^2F_{7/2})_1$	$4\times T^{1.8}$	40∼70	FLN	9
14	ZBLAN	Nd^{3+}	$^4I_{9/2} \rightarrow {}^7F_{3/2}$	$\propto T^{1.1\pm0.1}$	1.4∼8	SHB	34
15	Fused silica	Nd^{3+}	$^4I_{9/2} \rightarrow {}^7F_{3/2}$	$3.5\times T^{1.3}$	0.05∼1	PE	35
16	Silicate	Eu^{3+}	$^5D_0 \rightarrow {}^7F_0$	$9\times T^{1.0\pm0.1}$	0.4∼4.2	SHB	36
17	Silicate	Pr^{3+}	$^1D_2 \rightarrow {}^3H_4$	$30\times T^{1.3\pm0.1}$	0.4∼12	SHB	36

[a]FLN=fluorescence line narrowing, SHB=spectral hole burning, PE=photon echoes.

in ZBLA.[7] This seems consistent with the findings that the electron-phonon coupling strength is stronger for actinide ions than lanthanide ions, because of larger mixing of $5f^{n-1}6d$ states due to the stronger LS coupling;[21,22] and the electron-phonon coupling is stronger for Yb^{3+} ($4f^{13}$) than Eu^{3+} ($4f^6$), because of the combination of the effects of the lanthanide contraction, the screening of the $4f$ electrons, and the position of the opposite parity states ($4f^{n-1}\,5d$).[23] For the $(^2F_{5/2})_1 \rightarrow (^2F_{7/2})_1$ transition of Yb^{3+} ions, the homogeneous widths were reported to be $15\times T^{1.3}$ and $4\times T^{1.8}$ in phosphate glass from 6.5 to 70 K with a crossover at ∼40 K by FLN (Ref. 9) (rows 12, 13). The possible reasons for the difference below 40 K, are that Yb^{3+} ions coupling to the lattice is so weak in phosphate glass that TLS's dominate even at a temperature of 40 K;[24] or that the instrumental resolution in that measurement was not sufficient to fully resolve the homogeneous linewidth at temperatures below 40 K.[25] Our results are about three times larger than that of $4\times T^{1.8}$ above 40 K. This difference may be ascribed to the higher density of states of low-energy phonons in fluorozirconate glasses. The last group (rows 14–17) lists the measurements at low temperature ($T\leqslant 12$ K) by spectral hole-burning and photon echo techniques, which have demonstrated linear and $T^{1.3}$ dependencies on temperature. In some of the published studies, there are reports of variation in measured homogeneous linewidth across the inhomogeneous profile in addition to instrumental or other artifacts, presumably due to the site-dependent electron-phonon coupling strengths. In ZBLA:Eu^{3+}, for example, choice of different excitation wavelengths led to a factor of 2 change in homogeneous linewidth.[7]

The nearly T^2 dependence of the homogeneous linewidth of the transition between the lowest Stark levels is characteristic of a two-phonon Raman process. However, the persistence of the behavior down to a temperature as low as 10 K, in our measurements and those in the second and third groups of Table I, seems to rule out the Raman mechanism. To explain the anomalous T^2 behavior, Huber[26] has pointed out an effective Debye cutoff frequency in inorganic glasses, based on the maximum in the density of states. It could be up to ten times lower than the nominal Debye frequency of the glass. By modifying the density of states, the high temperature T^2 behavior can be expected to extend to correspondingly much lower temperature than in crystalline systems. This temperature range may extend down to 10 K. An alternative approach to this issue is the fracton description of Dixon and co-workers.[27] This approach involves a range of length scales for which the geometric structure of a disordered system is self-similar. The consequence of this self-similarity leads to a $\omega^{1/3}$ for the density of states of localized vibrational modes (fractons) instead of ω^{d-1} for that of Debye phonons (d is Euclidean dimension).[28,29] The T^2 dependence has been obtained in the temperature range 10–300 K by using the McCumber-Sturge formulation[30] and considering the dephasing of the optical transition in Raman processes via a two-fracton instead of a two-phonon interaction.

B. Inhomogeneous linewidths

The inhomogeneous widths in Figs. 5 and 6 were nearly constant with temperature, and therefore dominate at low temperature. These inhomogeneous widths, $\Delta\overline{\nu_G}\sim$(33.1

$\pm 1.4)$ cm^{-1} in emission and $\Delta\overline{\nu}_G \sim 23.6 \pm 0.6$ cm^{-1} in absorption, are smaller than in most oxide glasses. This is likely the consequence of Yb^{3+} ions substituting for the glass-forming cations, which have a well-defined coordination and experience small variations from site to site in the local crystal field.[31] The reasons for the difference in inhomogeneous linewidths between ~ 33.1 cm^{-1} in emission and ~ 23.6 cm^{-1} in absorption are unclear. The inhomogeneous linewidths have been reported to be excitation dependent in fluorozirconate glasses at low temperature, and the values we find for the inhomogenous widths are comparable to those found in similar systems. Two distinct types of site distributions with the inhomogeneous linewidths of 33 cm^{-1} and 18 cm^{-1} have been observed by Adam *et al.*[31] in ZBL:Eu^{3+} measured by a dye-laser excitation spectra of the $^5D_0 \rightarrow {}^7F_0$ transition at 4.4 K. The first linewidth of 33 cm^{-1} agrees with the value of ~ 33.1 cm^{-1} from our emission data. This value of inhomogeneous width (half width at half maximum) was also reported in ZB:Nd^{3+} between the lowest Stark levels of the $^4I_{9/2}$ and $^4I_{3/2}$ manifolds from absorption spectrum at 4.2 K.[6] With time-resolved site-selective emission spectra of the $^5D_0 \rightarrow {}^7F_{0,1}$ transitions in ZBLAN:Eu^{3+} at 10 K, Balda *et al.*[32] reported that a narrowed excitation spectra with a width of 23 cm^{-1} at high energy side of the $^5D_0 \rightarrow {}^7F_1$ transition, and as the collecting wavelength increases, the width broadened to 42 cm^{-1}. They concluded that the effect is due to coincidental emission from two Eu^{3+} sites. The initially narrowed width of 23 cm^{-1} is close to the value from our absorption data. On the other hand, Harrison and co-workers[16,33] argued that the extra features visible in some of these spectra are not due to two different site distributions, but is a single site distribution in ZBLANP:Eu^{3+} distorted by simultaneous excitation into its phonon side band.

IV. CONCLUSION

We use Voigt profiles to deconvolute the homogeneous and inhomogeneous linewidths of the $(^2F_{5/2})_1 - (^2F_{7/2})_1$ transitions in Yb^{3+}-doped ZBLANP glass between 10 and 300 K. The emission and absorption spectra of Yb^{3+} ion in ZBLANP offer nearly isolated $(^2F_{5/2})_1 - (^2F_{7/2})_1$ transitions that lend themselves to mathematical deconvolution of the Voigt profiles. The inhomogeneous widths show a value nearly constant with temperature as expected. The $T^{1.9}$ dependence of homogeneous linewidth was similar to that observed in other rare-earth-doped systems studied by FLN and photon echoes, but in contrast to the result in Yb^{3+}-doped phosphate glass which showed a $T^{1.3}$ dependence below 40 K. Our data do not suggest a crossover between two different dephasing mechanisms (e.g., TLS and two-phonon) in the temperature range studied, but add to a growing body of results that show a T^2 dependence. Further experiments below 10 K would be worthwhile in the search for the crossover. This deconvolution technique allows one to measure both homogeneous and inhomogeneous linewidths at the same time and is capable of covering a broad range of temperatures. The deconvolution technique is applicable for spectral linewidth studies where a transition peak can be well resolved.

ACKNOWLEDGMENTS

The authors would like to thank Dr. C. W. Wilkerson, Jr. for helpful discussions, and Dr. W. C. Danen for his support on this project. This work has been carried out under the auspices of the U.S. Department of Energy.

[1] *Optical Linewidths in Glasses*, edited by M. J. Weber [special volume, J. Lumin. **35** (1987)].
[2] *Optical Spectroscopy of Glasses*, edited by I. Zschokke (Reidel, Dordrecht, 1986).
[3] P. W. Anderson, B. I. Halperin, and C. M. Varma, Philos. Mag. **25**, 1 (1972).
[4] W. A. Philips, J. Low Temp. Phys. **7**, 351 (1972).
[5] J. Hegarty and W. M. Yen, Phys. Rev. Lett. **43**, 1126 (1979).
[6] J. M. Pellegrino, W. M. Yen, and M. J. Weber, J. Appl. Phys. **51**, 6332 (1980).
[7] F. Durville, G. S. Dixon, and R. C. Powell, J. Lumin. **36**, 221 (1987).
[8] R. T. Brundage, R. L. Powell, J. V. Beitz, and G. K. Liu, J. Lumin. **69**, 121 (1996).
[9] R. T. Brundage and W. M. Yen, Phys. Rev. B **33**, 4436 (1986).
[10] R. T. Brundage and C. S. Reyerson, Phys. Rev. B **53**, R8821 (1996).
[11] P. M. Selzer, D. L. Huber, D. S. Hamilton, W. M. Yen, and M. J. Weber, Phys. Rev. Lett. **36**, 813 (1976).
[12] *Persistent Spectral Hole-Burning: Science and Applications, Vol. 44*, edited by W. E. Moerner (Springer-Verlag, Berlin, 1988).
[13] R. M. Shelby, Opt. Lett. **8**, 88 (1983).
[14] R. I. Epstein, M. I. Buchwald, B. C. Edwards, T. R. Gosnell, and C. E. Mungan, Nature (London) **377**, 500 (1995).
[15] K. Tanimura, M. D. Shinn, W. A. Sibley, M. G. Drexhage, and R. N. Brown, Phys. Rev. B **30**, 2429 (1984).
[16] M. T. Harrison, R. G. Denning, and S. T. Davey, J. Non-Cryst. Solids **184**, 286 (1995).
[17] T. Kushida and E. Takushi, Phys. Rev. B **12**, 824 (1975).
[18] B. Di Bartolo, *Optical Interactions in Solids* (Wiley, New York, 1968).
[19] F. Schreier, J. Quant. Spectrosc. Radiat. Transf. **48**, 743 (1992).
[20] J. Humlicek, J. Quant. Spectrosc. Radiat. Transf. **27**, 437 (1982).
[21] M. C. Williams and R. T. Brundage, Phys. Rev. B **45**, 4561 (1992).
[22] J. P. Hessler, R. T. Brundage, J. Hegarty, and W. M. Yen, Opt. Lett. **5**, 348 (1980).
[23] A. Ellens, H. Andres, M. L. H. t. Heerdt, R. T. Wegh, A. Meijerink, and G. Blasse, J. Lumin. **66&67**, 240 (1996).
[24] W. M. Yen and R. T. Brundage, J. Lumin. **36**, 209 (1987).
[25] R. M. Macfarlane and R. M. Shelby, J. Lumin. **36**, 179 (1987).
[26] D. L. Huber, J. Non-Cryst. Solids **51**, 241 (1982).

[27] G. S. Dixon, R. C. Powell, and G. Xu, Phys. Rev. B **33**, 2713 (1986).
[28] S. Alexander, C. Laermans, R. Orbach, and H. M. Rosenberg, Phys. Rev. B **28**, 4615 (1983).
[29] S. K. Lyo and R. Orbach, Phys. Rev. B **29**, 2300 (1984).
[30] D. E. McCumber and M. D. Sturge, J. Appl. Phys. **34**, 1682 (1963).
[31] J. L. Adam, V. Poncon, J. Lucas, and G. Boulon, J. Non-Cryst. Solids **91**, 191 (1987).
[32] R. Balda, J. Fernandez, H. Eilers, and W. M. Yen, J. Lumin. **184**, 286 (1995).
[33] M. T. Harrison and R. G. Denning, J. Lumin. **69**, 265 (1996).
[34] R. M. Macfarlane and B. Jacquier, J. Non-Cryst. Solids **161**, 254 (1993).
[35] M. M. Broer, B. Golding, W. H. Haemmerle, J. R. Simpson, and D. L. Huber, Phys. Rev. B **33**, 4160 (1986).
[36] T. Schmidt, R. M. Macfarlane, and S. Volker, Phys. Rev. B **51**, 15 707 (1994).